

## An Approximate Model Describing Electrospinning of Nanofibers: Process Parameter Investigation

*Panu Danwanichakul<sup>\*</sup>, Duangkamol Dechojarassri & Ramida Werathirachot*

*Department of Chemical Engineering, Faculty of Engineering, Thammasat University,  
99 Moo 18 Khlong Nung, Khlong Luang, Patumthani 12120, Thailand*

---

**Abstract:** *A mathematical model of electrospinning process using poly(vinyl alcohol) as a model material was explained to investigate the effect of process parameters on the nanofiber diameter. These parameters include the needle diameter, the applied voltage, the distance between the needle tip and the plate collector, and the angle of needle with respect to the vertical axis. It was found that when increasing the needle diameter, increasing the tip-to-collector distance, increasing the angle of the needle, or lowering the voltage, the PVA nanofiber diameter was increased.*

**Keywords:** *Electrospinning, PVA, poly (vinyl alcohol), process parameter, nanofiber*

---

### 1. INTRODUCTION

Electrospinning is now known for its easiness in producing submicron fibers and fabricating nanofibrous membranes which have been used in biomedical engineering such as scaffolds for tissue growth [1], wound dressing [2], and drug releases [3, 4]. Nanostructures are anticipated to give exceptionally high performance attributable to their large surface area per unit mass. Even though electrospinning has not been practical in large scale production yet, the number of basic researches on electrospinning is now increasing rapidly. Using electrospinning technique, many polymers have been investigated whether they could be shaped as nanofibers from either melts or solutions. One of the most studied polymers is poly(vinyl alcohol) or PVA. Thus far, not only has PVA been studied for biomedical purposes, but it has also been used in the preparation of nanocrystals [5]. Many factors influencing PVA nanofiber morphology, both process parameters and solution parameters, have been reported. Process parameters are the applied voltage of the power supply [4, 6] and the tip-to-collector distance [4, 6]. What are considered as solution parameters are the degree of hydrolysis of PVA [4, 7], the molecular weight of PVA [7], the solution concentration [4], the solution pH [8], other ions in the solutions [4], and the types of solvents [4].

Although the electrospinning process itself is easy to handle experimentally, the process modeling is very complicated. Yarin *et al.* (2001) [9] modeled the change of liquid droplet shape while the electrical voltage was applied prior to the flight of liquid

---

<sup>\*</sup>corresponding author: dpanu@tu.ac.th

jet. They found that Taylor cone did not represent a unique critical shape and it was shown both theoretically and experimentally that a critical shape was the shape of a cone with half angle of  $33.5^\circ$ , rather than a cone of  $49.3^\circ$ . Many groups have attempted to explain the stretching of ultrafine fibers. Reneker *et al.* (2000) [10] studied the bending instability in electrospinning by observing in the experiments together with modeling the liquid jet motion using viscoelastic model in one dimension and three dimensions. The polymer solution jet was considered as viscoelastic dumbbell of which one bead was fixed by non-Coulomb force and the other was accelerated according to the Coulomb repulsive force from the electric field and between two beads. The three dimension model was qualitatively successful in predicting the behavior of stretching a fiber into a spiral loop while reaching the collector. The effect of bending instability was also observed by Shin *et al.* (2001) [11]. They proposed the operating diagrams of glycerol and polyethylene oxide (PEO) -water systems explicating the regions of the jet behaviors as a function of the electric field and flow rate. They found that there was a transition coincided with the onset of instability. Below a specific value of electric field strength (KV/cm), the jet was stable and follows a straight path and above that, the jet started bending, which finally turned into a whipping motion. The comparison was made between experimental and theoretical results. Moreover, Feng (2003) [12] explored the stretching of charged jet in view of fluid mechanics and rheology, and the role of viscoelasticity. Theron *et al.* (2004) [6] experimented with PVA, PEO, and other polymers. They correlated the governing parameters which are the applied voltage, the solution flow rate, the polymer concentration, the nozzle to ground distance, and the concentration of ethanol in solution with charge density as an empirical equation. To capture the essence of electrospinning with simple correlations, scaling laws were also proposed. Based on balance equations of current and forces, with an aid of allometric approach, the power law between electric current and solution flow rate was obtained [13]. In addition, for the case when charged jet can be regarded as an Ohmic conductor, the relation between the electric current and applied voltage was expressed as a power law [14].

In the present work, an approximate model based on Newton's law of motion is proposed to study the effect of process parameters in electrospinning process using PVA as a model polymer. Together with the effect of voltage and the tip-to-collector distance, which have been studied extensively, other process parameters were investigated including the tip diameter and the angle between tip and vertical axis. The next section, Section 2, explains typical experimental set-up of electrospinning process. Section 3 gives the detail of the model while Section 4 provides the results along with the discussions. Finally, the conclusion is made in Section 5.

## 2. MATERIALS AND METHODS

PVA used in this research was purchased from Sigma Aldrich. It is a cold water soluble type with molecular weight ( $M_w$ ) of 40,000-70,000 and degree of hydrolysis of 98%. The concentration of PVA in aqueous solution was fixed at 30% wt/vol throughout the experiments.

### An Approximate Model Describing Electrospinning of Nanofibers:

Electrospinning equipment is composed of a high voltage power supply, an acrylic plate covered with aluminum foil as a collector and placed on an adjustable vertical stand, a glass syringe with a metal needle, and a bar with a hole to place the syringe at a fixed inclination. The positive electrode is placed at the needle tip and the ground is placed at the collector. The length of all needles used is 3.5 cm and the spinning time was held constant at 5 min for all experiments. Other parameters may be changed for the investigation.

The morphology of an electrospun sample is obtained with a scanning electron microscope (SEM, modeled JEOL, JSM-6301F). All specimens were coated by gold using Gold Sputtering Coater (modeled JEOL, JFC-1200 fine coater) before being investigated with SEM. The SEM micrograph was later checked with an image analyzer program in order to measure the size of produced fibers.

### 3. A DESCRIPTION BASED ON NEWTON'S LAW OF MOTION

In electrospinning process, a drop of solution at the needle tip is charged so the repulsive forces among charges were responsible for the transformation of the drop as well as the elongation to a continuous fiber. Our proposed theory here is focused on the initial stage of fiber formation which is the flow of spinning solution out of the capillary. The Newton's law of motion is adapted to explain the motion of the spinning fluid. To keep the derivation as simple as possible, many complications will be neglected altogether. For example, the derived equation will concern about the formation of smooth fibers only, not including bead-string fiber formation.

The force that initiates the flow is from charge electrostatic repulsion ( $F_e$ ) and it is counteracted with shear force ( $F_\mu$ ) at the capillary wall and the surface tension ( $F_\gamma$ ) at the periphery of the transforming drop. If we assume that the fluid would flow continuously to generate a continuous fiber, the cohesive forces resulting from the interaction of masses between the attached sections would be cancelled. In addition, the electrical force is considered much greater than the gravity force. Therefore, the equation can be expressed as

$$F_e - F_\gamma - F_\mu = m \frac{dv_{av}}{dt}, \quad (1)$$

where  $m$  is the controlled mass of the spinning fluid and  $v_{av}$  is the average velocity. Each term on the left-handed side is written as follows.

$$F_e = k_1 \frac{V \cos \theta}{H} + k_2 \sigma \quad (2)$$

$$F_\gamma = k_3 \gamma \pi D_n \quad (3)$$

$$F_\mu = k_4 \pi D_n L \tau_{rz} = k_4 \pi D_n L \left( -\mu \frac{dv_z}{dr} \right) \quad (4)$$

All  $k$ 's are the constants. In Eq. (2), the electrical force from charge repulsions is assumed dependent on electric field  $\left( \frac{V \cos \theta}{H} \right)$ , where  $V$  is the applied voltage from the

power supply,  $H$  is the distance between the tip measured perpendicular to the collector, and  $\theta$  is the angle between the needle and the vertical axis, and also on the conductivity of the spinning solution. Eq. (3) is related to surface tension ( $\gamma$ ) and the perimeter of the surface,  $\pi D_n$ , in which  $D_n$  is the needle diameter. Eq. (4) represents shear force which is the product of shear stress ( $\tau_{rz}$ ) and the surface area of the needle wall,  $\pi D_n L$ , where  $L$  is the length of the needle. For simplicity, we assume that the spinning solution is Newtonian fluid. The equation is then simplified to

$$F_\mu = k_4 \pi D_n L \left( \mu \frac{v_{av}}{R_n} \right) = 2k_4 \pi L \mu v_{av} \quad (5)$$

Where,  $\mu$  is the solution viscosity and the velocity gradient  $-\frac{dv_z}{dr}$  is approximated as the average velocity divided by the radius of the needle. Therefore, Eq. (1) becomes

$$\left( k_1 \frac{V \cos \theta}{H} + k_2 \sigma \right) - k_3 \gamma \pi D_n - 2k_4 \pi L \mu v_{av} = m \frac{dv_{av}}{dt} \quad (6)$$

Upon solving Eq. (6) with an initial condition;  $t = 0, v_{av} = 0$ , we get

$$v_{av} = \frac{\left( k_1 \frac{V \cos \theta}{H} + k_2 \sigma \right) - k_3 \gamma \pi D_n}{2k_4 \pi L \mu} \left[ 1 - e^{-\frac{2k_4 \pi L \mu t}{m}} \right] \quad (7)$$

The flight of the solution jet out of the needle tip has an average velocity according to Eq. (7). The fluid is initially at rest and then the average velocity increases and finally reaches a constant at large time which is at steady state. While the jet travels, the mass will be elongated. To conserve the mass  $m$ , the diameter of the fiber  $D$  is decreased upon elongation. If the mass of the control volume,  $m = \frac{\pi}{4} D^2 l \rho$ , where  $\rho$  is the density of fluid,  $l$  is the assumed length of small cylindrical section of fluid, the average velocity which is also the velocity of the moving front of fluid is

$$v_{av} = \frac{dl}{dt} = \frac{-8m}{\pi \rho} \frac{1}{D^3} \frac{dD}{dt} \quad (8)$$

Equate eq. (7) and Eq. (8), we get

$$\frac{-2}{D^3} \frac{dD}{dt} = \frac{\left( k_1 \rho \frac{V \cos \theta}{H} + k_2 \sigma \rho \right) - k_3 \gamma \pi \rho D_n}{8k_4 L \mu m} \left[ 1 - e^{-\frac{2k_4 \pi L \mu t}{m}} \right] \quad (9)$$

Integrating Eq. (9) with the condition,  $D(t = 0) = D_n$ , we obtain the relation,

$$\frac{1}{D^2} = \frac{1}{D_n^2} + \frac{\left( k_1 \rho \frac{V \cos \theta}{H} + k_2 \sigma \rho \right) - k_3 \gamma \pi \rho D_n}{8k_4 L \mu m} \left[ t - \frac{me^{-\frac{2k_4 \pi L \mu t}{m}}}{2k_4 \pi L \mu} \right] \quad (10)$$

### An Approximate Model Describing Electrospinning of Nanofibers:

Since  $D_n \gg D$ , Eq.(10) is further simplified to

$$\frac{1}{D^2} = \frac{(k_1 \rho \frac{V \cos \theta}{H} + k_2 \sigma \rho) - k_3 \gamma \pi \rho D_n}{8k_4 L \mu m} \left[ t - \frac{me \frac{2k_4 \pi L \mu t}{m}}{2k_4 \pi L \mu} \right] \quad (11)$$

Actually, the process of fiber elongation is intrinsically complex. As was explained by some literature, for example, Reneker *et al* (2000) [10], the fiber formation would undergo bending instability and develop the spiral cone envelop. This enhances the distance for a fiber to extend. In addition, splitting and splaying may be involved in nanofiber formation. He *et al.* [15] proposed a critical length of straight jet in electrospinning. It is the length of the jet where the bending instability begins. The minimum value of nanofiber radius at the instability point could be correlated with the

square root of the length. Considering Eq. (8), we could also get that  $D \propto \frac{1}{\sqrt{l}}$ , from the conservation of mass. In the next section, the validity of Eq. (11) is checked with the experimental results provided.

### 3. RESULTS AND DISCUSSIONS

The properties of PVA solution were first measured. The viscosity of the PVA solution was 2641 cP, the surface tension was 77.9 mN/m, and the electrical conductivity was 1.833 mS/cm. The viscosity is high enough to ascertain the outcome of smooth fibers rather than bead-string fibers. These properties are the same for all experiments in this work. The following subsections provide the results of the electrospinning process.

#### 3.1 The Effect of Needle Diameter

The micrographs of electrospun fibers using various needle diameters from 0.6 to 1.1 mm, whereas other parameters were fixed are shown in Figure 1 along with their size distributions. The voltage used was 18 kV and the tip-to-collector distance was 9 cm. The needle was set perpendicular to the collector (0 degree). The average size of PVA fibers is seen to decrease when the needle diameter increases. Figure 2 shows the linear

relation between  $\frac{1}{D^2}$  and  $D_n$ . The slope is negative as was shown by Eq. (11) and it is related to the surface tension of the solution. As the size of the needle increases, the droplet size at the tip increases, yielding higher effect from surface tension. While the electrical force was kept the same, increasing surface tension effect would increase the size of the fibers.

#### 3.2 The Effect of the Applied Voltage

Figure 3 shows the micrographs of nanofibers generated under the effect of different voltage while keeping other factors constant. The voltage was varied between 9 and 24 kV while the tip-to-collector distance was 9 cm. The needle was set perpendicular to the

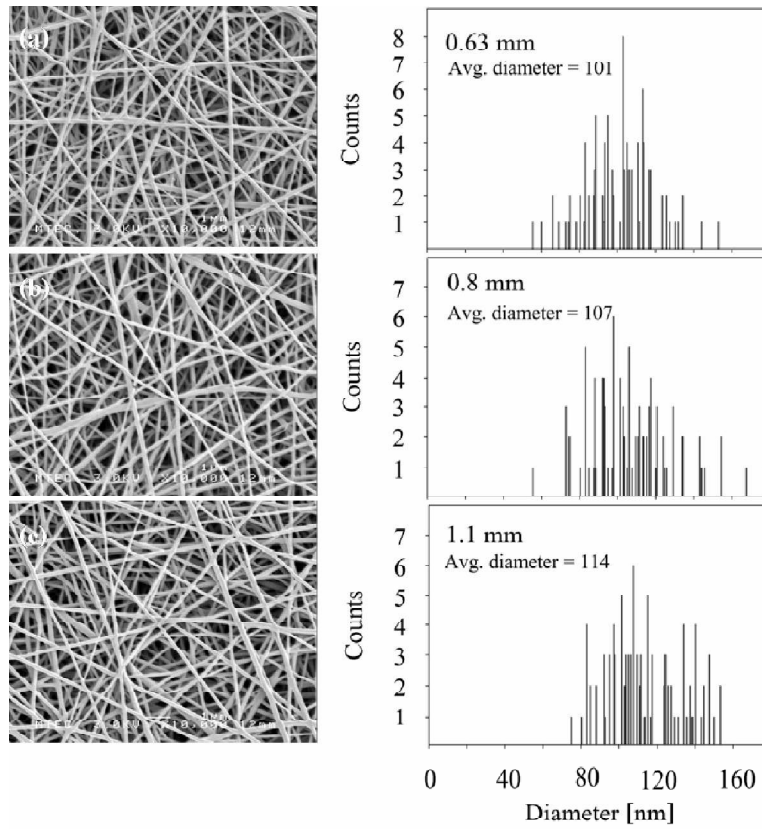


Figure 1: Micrographs of Electrospun PVA Nanofibers Comparing the Effect of the Needle Diameter,  $D_n$ . The Size Distributions and the Average Sizes are also Shown

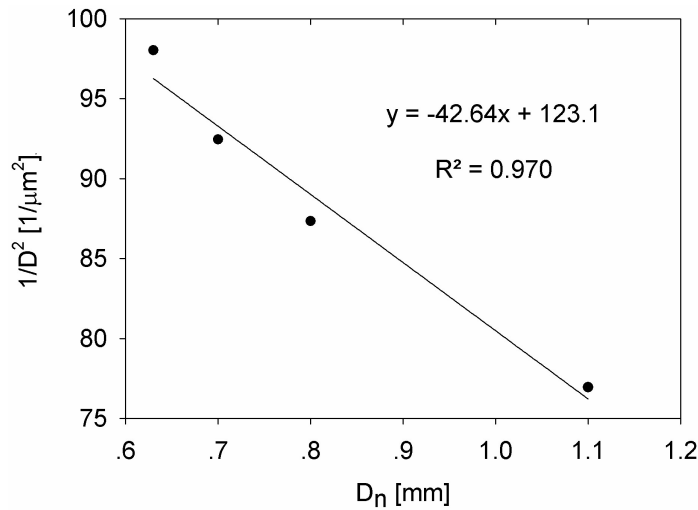
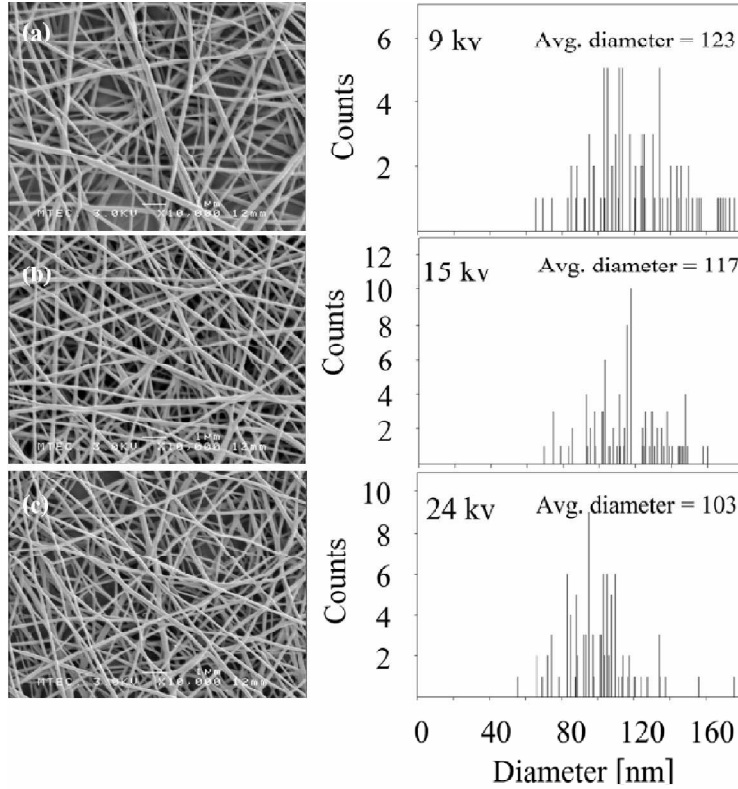


Figure 2: The Relation between  $1/D^2$  and the Diameter of the Needle,  $D_n$

### An Approximate Model Describing Electrospinning of Nanofibers:



**Figure 3: Micrographs of Electrospun PVA Nanofibers Comparing the effect of the Applied Voltage,  $V$ . The Size Distributions and the Average Sizes are also Shown**

collector (0 degree). The linear plot between  $\frac{1}{D^2}$  and  $V$  is shown in Figure 4. While the tip-to-collector distance is the same, increasing the voltage will increase electric field strength, resulting in increasing the electrical force. Theron *et al.* [6] showed that  $q \propto V^n$ , where  $q$  is the charge density,  $V$  is the voltage and the index  $n$  is a constant. The charge density is believed responsible for the charge repulsive forces stretching fibers to nanosize range. Similar relation was proposed by He *et al.* [14]. They stated the relation between electric current and applied voltage by a scaling law.

Our finding is different from what was reported by Zhang *et al.* [4]. They found that the average diameter of the fibers increased with the applied voltage. However, the broader size distribution was seen at higher voltage. This difference may come from the value of the voltage and the tip-to-collector distance used. They varied the voltage between 5 to 13 kV and fixed the distance at 15 cm. Their electric field strength was less than unity while ours was greater. The electric field strength less than unity might be too small to maintain the continuous formation of nanofibers, as was seen in their SEM figures that the number of fibers shown were very few to obtain good statistics.

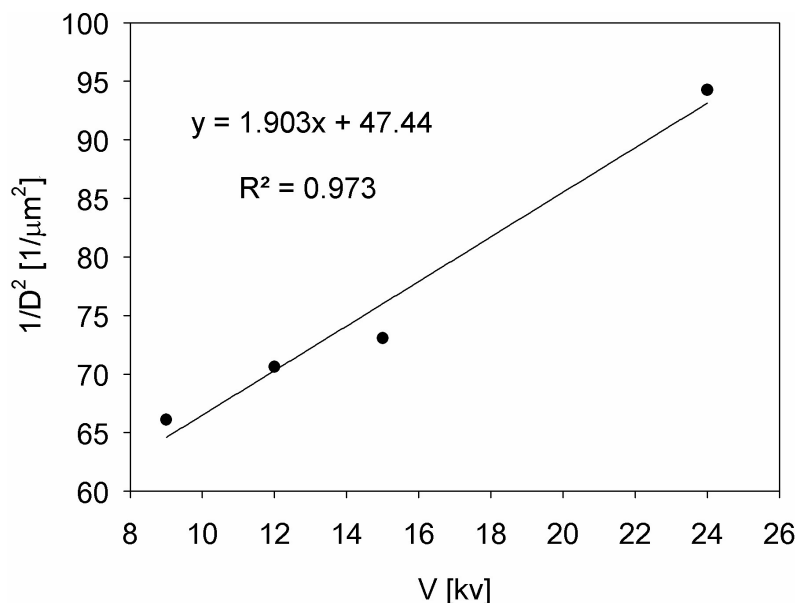


Figure 4: The Relation between  $1/D^2$  and the Voltage of the Power Supply,  $V$

### 3.3 The Effect of the Distance between the Needle tip and the Collector

The distance between the needle tip and the plate collector was found to affect the nanofiber size as shown in Figure 5. The distance was varied from 6 cm to 18 cm. The voltage was held constant at 18 kV and the needle was set perpendicular to the collector (0 degree). When increasing this distance, the fiber diameter is seen increasing. When

plotting  $\frac{1}{D^2}$  versus  $\frac{1}{H}$  the linear relationship is obtained as shown in Figure 6. The

distance is related to the strength of the electric field. Increasing  $H$  will decrease the strength of the electric field, yielding the larger fibers. Unlike the effect of voltage, the strength of electric field in this case seems to affect the spinnability of the PVA fibers as well. It was seen that the spinnability, defined as the amount of fibers able to be spun from the solution, decreased when the strength of the electric field was decreased. This implies that the electrical force is too small to maintain the spinning of continuous fibers. The rate of solvent evaporation might be too rapid compared with the rate of elongation. When the solvent evaporates, the fiber is solidified and it is, thus, difficult to spin if the force is too little. Another cause might be from the less extent of repulsive forces. Larger  $H$  means the longer distance for a fiber to stretch and repulsive Coulomb force is inversely proportional to the distance between charges squared so the repulsive force is very weak when  $H$  is large.

It should also be noted that for the electrospinning of PEO solution [16], the minimum required electric field strength for continuous spinning was little affected by the distance between the nozzle and the target in a large range while in the short range is greatly



**An Approximate Model Describing Electrospinning of Nanofibers:**

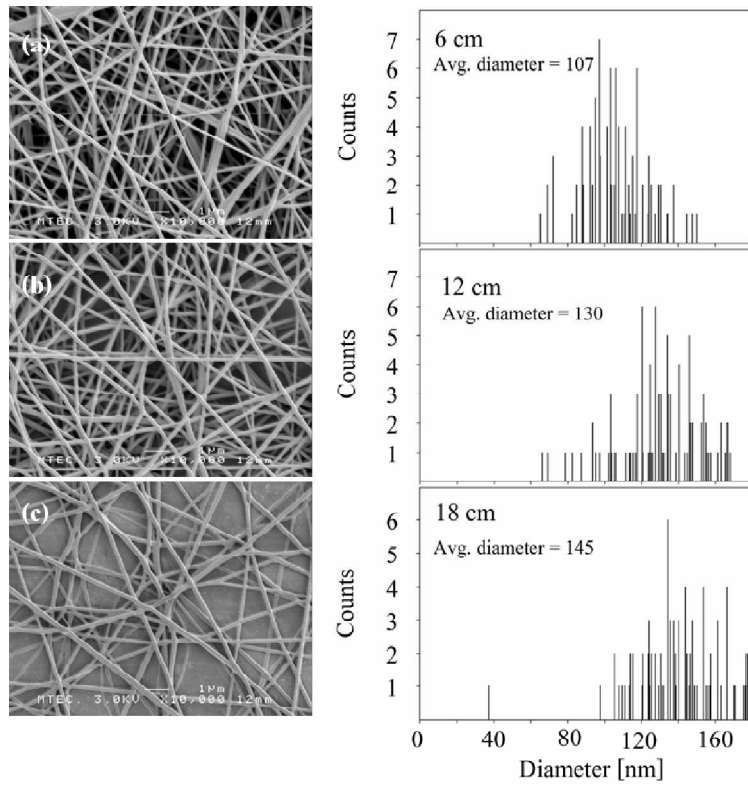


**Figure 5: Micrographs of Electrospun PVA Nanofibers Comparing the Effect of the tip-to-collector Distance,  $H$ . The Size Distributions and the Average Sizes are also Shown**

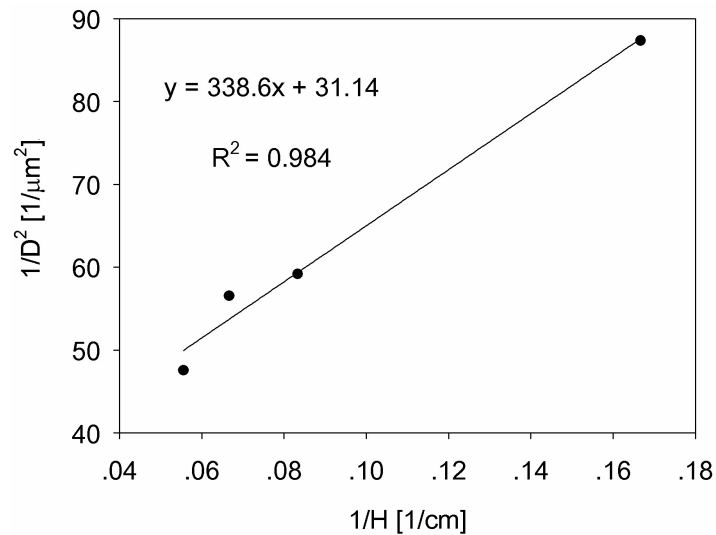


**Figure 6: The Relation between  $1/D^2$  and  $1/H$ ;  $H$  is the Distance between the Tip and the Plate Collector**

affected by the evaporation. In addition, the minimum required electric field was influenced by the flow rate at a large distance  $H$ .

### 3.4 The Effect of the Needle Inclination

The angle of the needle with respect to the vertical axis is closely related to the distance measured in the direction of the needle inclination between the tip and the collector. The angle was adjusted between  $15^\circ$  and  $75^\circ$  while the distance  $H$  was kept constant at 9 cm and the applied voltage was 18 kV. Therefore, the electric field in the direction of the needle is decreased when the angle is greater, resulting in larger fibers. The effect is

displayed in Figure 7 and the following plot between  $\frac{1}{D^2}$  and  $\cos(\theta)$  is shown in Figure 8. It can be observed that the correlation in Figure 8 is not good. This may be attributed to that the deposition of the fibers on the collectors was affected by the fluctuating distribution of electric field between the tip and the collector.

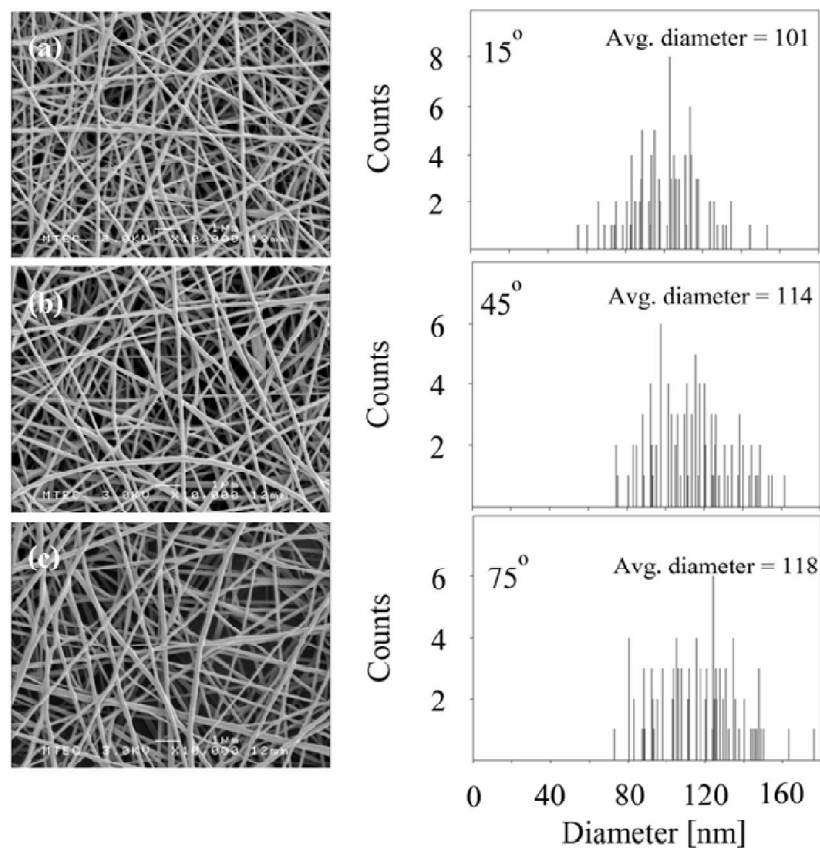


**Figure 7: Micrographs of Electrospun PVA Nanofibers Comparing the Effect of the Angle of the Needle with Respect to the Vertical Axis,  $\theta$ . The Size Distributions and the Average Sizes are also Shown**

### An Approximate Model Describing Electrospinning of Nanofibers:

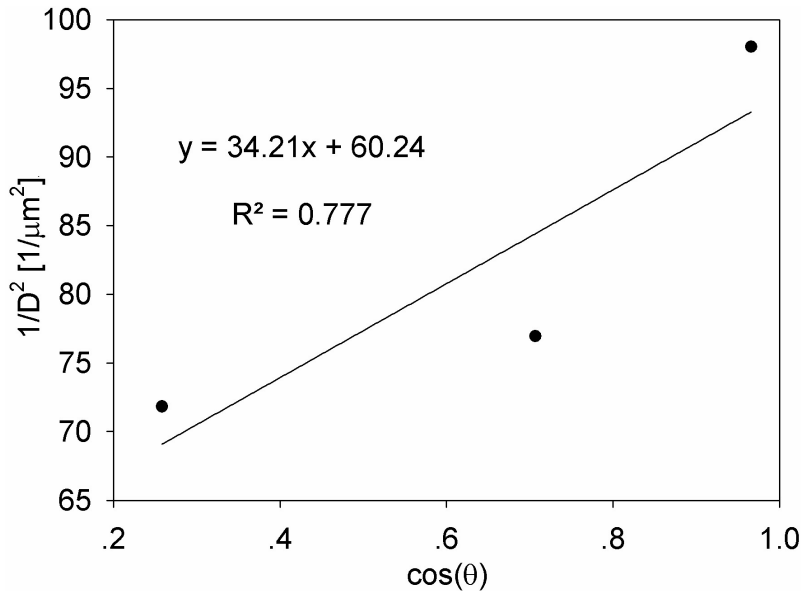


Figure 8: The Relation between  $1/D^2$  and  $\cos(\theta)$ ;  $\theta$  is the Angle between the Needle and the Vertical Axis

### CONCLUSIONS

An approximate model describing electrospinning of nanofibers was proposed based on Newton's law of motion. The process is actually very complicated as was observed experimentally by several groups. However, our model was made as simple as possible by neglecting all complications such as using only one-directional flow instead of extensional and viscoelastic flow, and assuming that a uniform fiber is stretched in one dimension instead of bending and splitting. Therefore, it could be useful in explaining the formation of smooth uniform nanofibers. More elaboration could be added later to improve the model and rigorous studies should be attempted next to explain the coefficients in the model. This model was checked first with the process parameters, which are the needle diameter, the applied voltage, the tip-to-collector distance and the angle of needle, with the experimental results of electrospinning of PVA and they were in good accord. Another ongoing research is investigating this model for the effect of solution parameters, which are the solution viscosity, conductivity and the surface tension.

### ACKNOWLEDGMENT

We are grateful to the Office of National Research Council of Thailand (NRCT) for financial support in the fiscal year 2007-2008.

### References

- [1] Duan B., Yuan X., Zhu Y., Zhang Y., Li X., Zhang Y., Yao K. Nanofibrous Composite Membrane of PLGA-chitosan/PVA Prepared by Electrospinning. *Euro Polym Jnl* 2006; **42**(9): 2013-2022.

- [2] Ignatova M., Starbova K., Markova N., Manolova N., Rashkov I. Electrospun Nano-fibre Mats with Antibacterial Properties from Quaternised Chitosan and Poly(vinyl alcohol). *Carbohydrate Res* 2006; **341**(12): 2098-2107.
- [3] Yang D., Li Y., Nie J. Preparation of Gelatin/PVA Nanofibers and their Potential Application in Controlled Release of Drugs. *Carbohydr Polym* 2007; **69**(3): 538-543.
- [4] Zhang C., Yuan X., Wu L., Han Y., Sheng J. Study on Morphology of Electrospun Poly(vinyl alcohol) Mats. *Euro Polym Jnl* 2005; **41**(3): 423-432.
- [5] Hong Y., Li D., Zheng J., Zou G. In Situ Growth of ZnO Nanocrystals from Solid Electrospun Nanofiber Matrixes. *Langmuir* **22** (17), 7331-7334.
- [6] Theron S. A., Zussman E., Yarin A. L. Experimental Investigation of the Governing Parameters in the Electrospinning of Polymer Solutions. *Polymer* 2004; **45**(6): 2017-2030.
- [7] Koshi A., Yim K., Shivkumar S. Effect of Molecular Weight on Fibrous PVA Produced by Electrospinning. *Mater Lett.* 2004; **58**(3-4): 493-497.
- [8] Son W. K., Youk J. H., Lee T. S., Park W. H. Effect of pH on Electrospinning of Poly(vinyl alcohol). *Mater Lett.* 2005; **59**(12): 1571-1575.
- [9] Yarin A. L., Koombhongse S., Reneker D. H. Taylor Cone and Jetting from Liquid Droplets in Electrospinning of Nanofibers. *J. Appl. Phys* 2001; **90**(9): 4836-4846.
- [10] Reneker D. H., Yarin, A. L., Fong H., Koombhongse S. Bending Instability of Electrically Charged Liquid Jets of Polymer Solutions in Electrospinning. *J. Appl. Phys* 2000; **87**(9): 4531-4547.
- [11] Shin Y. M., Hohman M. M., Brenner M. P., Rutledge G. C. Experimentally Characterization of Electrospinning: The Electrically forced Jet and Instabilities. *Polymer* 2001; **42**(25): 9955-9967.
- [12] Feng J. J. Stretching of a Straight Electrically Charged Viscoelastic Jet. *J. Non-Newtonian Fluid Mech.* 2003; **116**(1): 55-70.
- [13] He J. H., Wan Y. Q., Yu J. Y. Scaling Law in Electrospinning: Relationship between Electric Current and Solution Flow Rate, *Polymer* (2005); **46**(8): 2799-2801.
- [14] He J. H., Wan Y. Q. Allometric Scaling for Voltage and Current in Electrospinning, *Polymer* (2004); **45**(19): 6731-6734.
- [15] He J. H., Wu Y., Zuo W. W. Critical Length of Straight Jet in Electrospinning, *Polymer* (2005); **46**(26): 12637-12640.
- [16] Yang Y., Jia Z. D., Liu J. N., Wang L., Guan Z. The Effects of Flow Rate and the Distance between the Nozzle and the Target on the Operating Conditions of Electrospinning, *J. Polym. Eng.* (2008); **28**(1-2), 67-86.